

# Abstracts zur AG Seismologie (AK Auswertung/AK Wind und AK Technik)

## Montag - AK Auswertung

AG Seismologie, 21.-24.9.2019, Online-Meeting

### **Bericht über den Erdbebendienst des Bundes der BGR**

**K. Stammer**, M. Dohmann, T. Grasse, M. Hanneken, E. Hinz, M. Hoffmann,  
E. Muhire, L. Menke, C. Müller, R. Schönfelder, U. Stelling, E. Wetzig

Bundesanstalt für Geowissenschaften und Rohstoffe (BGR), Hannover

Es wird ein Überblick über die Tätigkeiten im technischen Bereich des Erdbebendienstes des Bundes der BGR gegeben. Der Bericht umfasst folgende Themen:

- Betrieb des GRSN, neue Standorte
- Ausbau der EIDA Netze
- abschließende Umbauarbeiten am GERES-Array
- seismologisches Datenzentrum der BGR, Noisebetrachtungen zur Qualitätskontrolle

## Neues vom Landeserdbebendienst Baden-Württemberg

Stefan Stange, Andrea Brüstle und Jens Zeiß

An der Netzwerkkonfiguration des LED in Baden-Württemberg hat sich im letzten Jahr nichts Grundsätzliches geändert. Bei der Systementwicklung wurde vor allem die Einbindung von SeisCompP3 (in Zukunft auch SeisCompP4) in das Auswertesystem voran getrieben. Die Detektionsempfindlichkeit wird mit Hilfe von Kreuzkorrelationsalgorithmen und dem MAGS-Detektor ständig weiter ausgebaut.

In den letzten zwölf Monaten wurden rund 950 lokale Erdbeben (BW und RLP) für das Bulletin manuell ausgewertet. Zehn davon konnten zusätzlich mit Hilfe der Antworten aus dem Kurzfragebogen makroseismisch bewertet werden. Für das stärkste Erdbeben (Magnitude  $ML=3.8$  am 4. November 2019 bei Albstadt) lieferten über 1500 erfasste Wahrnehmungsmeldungen eine Maximalintensität von V EMS. Ein weiteres, auf deutscher Seite in Kehl deutlich gespürtes Erdbeben gehörte zu einer ganzen Serie von induzierten Ereignissen, die mit der tiefen Geothermie Vendenheim nördlich von Strasbourg zusammen hingen. Das Geschehen dort wurde auch mit Mobilstationen begleitet.

Neben den bulletinwürdig lokalisierbaren Erdbeben wurde eine große Zahl von (sehr kleinen) sogenannten *Zählereignissen* detektiert bzw. identifiziert. Ein schönes Beispiel ist der Schwarm am Schneckenhaus bei Albstadt mit über 800 Ereignissen im September 2019, die noch vor wenigen Jahren weitgehend unentdeckt geblieben wären. Inzwischen werden diese Zählereignisse ebenfalls in der Bulletin-Datenbank des LED abgelegt. Eine Relativlokalisierung der stärkeren Schwarmbeben zeigte eine deutliche Ausrichtung in WNW-ESE-Richtung, also parallel zum Hohenzollergraben und nicht zur N-S-streichenden Albstadt-Scherzone.

Zum Thema *seismische Gefährdung* wurden mit dem ständig wachsenden Datensatz des LED bzw. des Erdbebendienstes Südwest weak-GMPEs für das Einzugsgebiet bestimmt. Besonderes Augenmerk lag dabei auf Stationskorrekturen und Effekten im Bereich des Nahfelds und der Moho-Reflexionen.

Ein weiterer Fokus lag und liegt auf Untersuchungen, die Aussagen zur Neotektonik oder zur Hintergrundseismizität bei tiefen Geothermie-Vorhaben im Oberrheingraben zum Ziel haben. So war der LED an einem gut dreiwöchigen Passiv-Seismik-Experiment im Kaiserstuhl beteiligt. Hoch gesampelte Daten von einem Dutzend Stationen auf engstem Raum wurden nach kleinsten Ereignissen auf vermeintlich aktiven Störungen (z.B. der Tuniberg-Störung) durchsucht. Hierzu wird auch gerade ein weiteres Experiment unter Federführung des KIT und der RWTH Aachen am Kandel (Waldkirchbeben von 2004) aufgezogen.



# Montag - AG Seismologie

## ICDP project Drilling the Eger Rift – brief activity report

Dahm T.<sup>1,2</sup>, Fischer T.<sup>3,4</sup>, Woith H.<sup>1</sup>, Hrubcová P.<sup>4</sup>, Kom M.<sup>5</sup>, Krueger F.<sup>2</sup>, Wagner, D.<sup>1,2</sup>, Horálek J.<sup>4</sup>, Vylita T.<sup>3</sup>, and the ICDP-Eger Science Team

<sup>1</sup>GFZ German Research Centre for Geosciences, Potsdam, Germany

<sup>2</sup>Institute of Geosciences, University of Potsdam, Germany

<sup>3</sup>Charles University, Faculty of Science, Prague, Czechia

<sup>4</sup>Institute of Geophysics, Czech Academy of Sciences, Prague, Czechia

<sup>5</sup>Institute of Geophysics and Geology, University of Leipzig, Germany

The ICDP-Eger drilling project develops a seismological lab at depth located in the western Eger Rift at the Czech-German border to enhance and study signals from micro-earthquakes and earthquake swarms in mid- to lower-crustal depth. In October 2016 the ICDP proposal was accepted for drilling four distributed, medium depth (<400 m) seismological monitoring wells S1-S4 and complementing two existing shallow wells (F1 and F2) at the CO<sub>2</sub> mofette at Hartoušov with a 239 m deep fluid and microbial activity monitoring well F3.

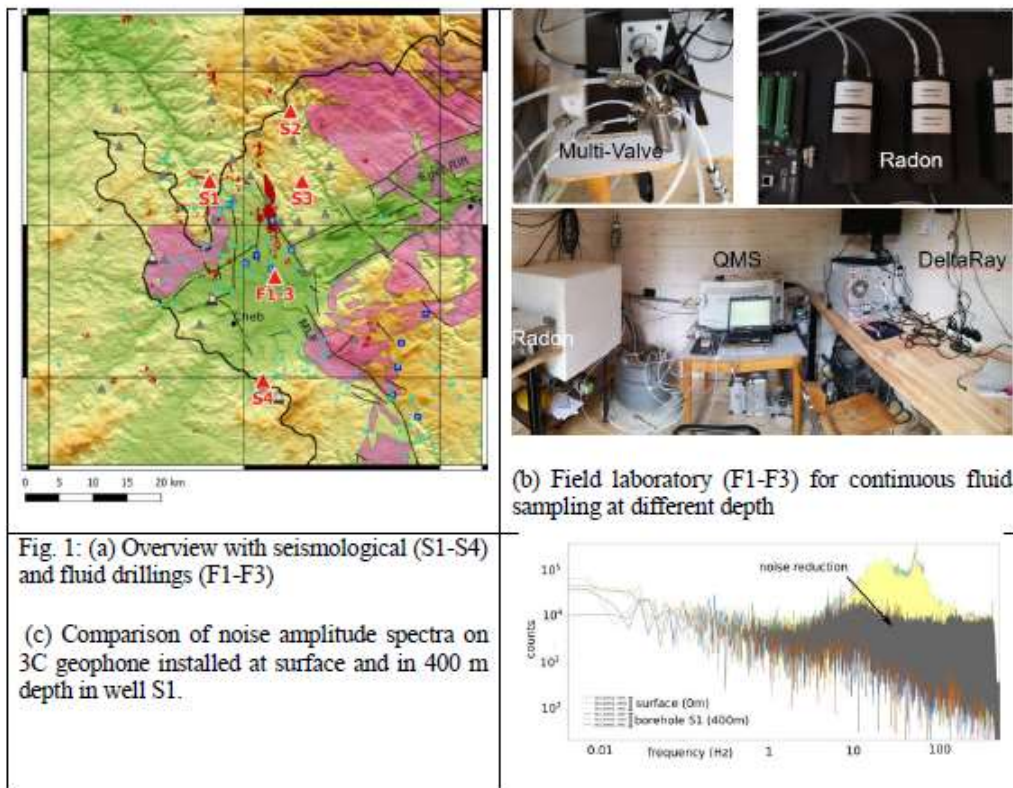


Fig. 1: (a) Overview with seismological (S1-S4) and fluid drillings (F1-F3)

(c) Comparison of noise amplitude spectra on 3C geophone installed at surface and in 400 m depth in well S1.

Drillings S1-S4 are planned for seismological monitoring. Instrumentation of the seismic wells S1-S3 include 8-element geophone chains and a bottom-hole wideband sensor. The borehole sensors at S1 will be complemented by small-aperture surface array of approximately 400 m diameter. A broadband surface station and a rotational sensor will complement the drilling.

The short presentation informs about the status of the project and drillings, sensor installation and the integration of monitoring and data handling.

## VSP Experiment am ICDP Bohrloch S1 in Landwüst, Vogtland

N. Lerbs<sup>1</sup>, K. Hannemann<sup>1</sup>, D. Domigall<sup>2</sup>, D. Vollmer<sup>2</sup>, M. Ohrnberger<sup>2</sup>, F. Krüger<sup>2</sup>, M. Korn<sup>1</sup>, T. Dahm<sup>2,3</sup>

<sup>1</sup> Universität Leipzig, Institut für Geophysik und Geologie, Leipzig, Deutschland,

<sup>2</sup> Universität Potsdam, Institut für Geowissenschaften, Potsdam, Deutschland,

<sup>3</sup> Deutsches GeoForschungsZentrum, Erdbeben- und Vulkanphysik, Potsdam, Deutschland

Das ICDP Projekt "Drilling the Eger Rift" befasst sich mit der Erforschung geodynamischer Prozesse in West-Böhmen/Vogtland, wie beispielsweise mit Schwarmbeben, Fluidkanälen und CO<sub>2</sub> Entgasungen in der Erdkruste. Im Zuge dessen wurden drei Bohrlöcher zur Installation von 3D seismischen Arrays erstellt. Eines dieser Bohrlöcher ist ca. 1.5 km südlich von Landwüst (Vogtland) entfernt und besitzt eine Tiefe von 402 m. Innerhalb dieses Bohrlochs ist eine Bohrlochkette mit 8 10 Hz 3-Komponenten Geophonen installiert sowie zusätzlich ein Oberflächenarray bestehend aus 12 4.5 Hz 3-Komponenten Geophonen geplant. Die seismischen Daten können mit einer Abtastrate von bis zu 1000 Hz aufgezeichnet werden.

Während des Bohrprozesses wurde eine bisher geologisch nicht erfasste, steil einfallende Störungszone in einer Tiefe von ca. 100 m – 160 m im Bohrkern identifiziert. Zur genaueren Charakterisierung des Untergrunds um das Bohrloch ist im Januar 2020 ein VSP (vertical seismic profiling) Experiment durchgeführt worden. Ziel des VSP Experiments ist die Charakterisierung der Störungszone und die Berechnung eines 2D-Geschwindigkeitsmodells des Untergrunds, das für die Lokalisierung der Fluidkanäle benötigt wird. Während des Experiments wurden die Sensoren der Bohrlochkette (8 10 Hz Geophonen) und 40 4.5 Hz 3-Komponenten Geophone als Oberflächenarray installiert. Das Oberflächenarray hatte eine Gesamtlänge von etwa 580 m. Der Abstand der Geophone betrug 20 m bzw. 40 m. Die Datenaufnahme erfolgte mit DataCubes und die Abtastrate während des Experiments betrug 400 Hz. Als Quellen kamen ein Fallgewicht (SDD 6600, 340 kg Fallgewicht, 2 m Fallhöhe, 40x40x3 cm Bodenplatte), ein Schussapparat (SISSY, Seismic Impulse Source SYstem) und eine mobile hochfrequente Vibrationsquelle (ELVIS, ELectrodynamic Vibrator System) zum Einsatz. Insgesamt wurden mit Hilfe der Vibrationsquelle 49 Quellpunkte und durch das Fallgewicht 64 Quellpunkte mit jeweils einem Abstand von 10 m angeregt.

Zur Berechnung des Geschwindigkeitsmodells wurden die Ersteinsätze der Fallgewichtquellen genutzt. Das Geschwindigkeitsmodell zeigt einen starken Kontrast zwischen oberflächennahen (Tiefe < 50 m) geringen Geschwindigkeiten (< 1500 m/s) und höheren Geschwindigkeiten (> 4000 m/s) bei zunehmender Tiefe. Zudem ist eine NW-SE einfallende Zone verringerter Geschwindigkeit sichtbar, die das Bohrloch bei ca. 90 m – 170 m schneidet. Diese Geschwindigkeitsanomalie kann mit der bei der Bohrung identifizierten Störungszone oder durch den Lithologiewechsel von Muskovitphyllit zu Schluffphyllit in Zusammenhang stehen.



## Multi-level gas monitoring to study fluid-earthquake-interactions

Heiko Woith<sup>1</sup>, Kyriaki Daskalopoulou<sup>1</sup>, Martin Zimmer<sup>1</sup>, Tomáš Fischer<sup>2</sup>, Josef Vlček<sup>2</sup>,  
Jakub Trubač<sup>2</sup>, Jan-Erik Rosberg<sup>3</sup>, Tomáš Vylita<sup>2</sup>, Torsten Dahm<sup>1</sup>

<sup>1</sup> GFZ German Research Centre for Geosciences, Potsdam, Germany

<sup>2</sup> Charles University, Faculty of Science, Prague, Czech Republic

<sup>3</sup> Lund University, Sweden

A new approach to monitor geochemical and geophysical fluid properties at different depth levels is presented. This setup can provide hints on the origin of temporal variations, as the velocity and direction of migrating fluids can be measured directly. In the frame of the ICDP-project "Drilling the Eger Rift: Magmatic fluids driving the earthquake swarms and the deep biosphere" a prototype of such a multi-level gas monitoring system has been setup at the Hartoušov mofette field which is located in the Cheb Basin (West Bohemia) and is known for intense mantle-CO<sub>2</sub> degassing and nearby recurring earthquake swarms. The mofette is believed a gas emission site where CO<sub>2</sub> ascends from as deep as the upper mantle, and may therefore provide a natural window to ongoing magmatic processes at mantle depth. Fluids from three adjacent boreholes - 30 m, 70 m, and 230 m deep - will be continuously monitored at high sampling rates. The instrumentation comprises flow and pressure probes, as well as devices to monitor fluid-geochemical properties and stable isotopes. Additional to the gas monitoring equipment, the following instruments are installed: a weather station, a broadband seismometer at the surface, and a borehole seismometer at 70 m depth. We present the technical setup and first results obtained during the drilling of the deepest borehole.

## High frequency array observations at surface and borehole stations at ICDP Eger Rift site Landwüst (Vogtland)

K. Hannemann<sup>1</sup>, D. Domigall<sup>2</sup>, M. Ohrberger<sup>2</sup>, N. Lerbs<sup>1</sup>, D. Vollmer<sup>2</sup>, F. Krüger<sup>2</sup>, M. Korn<sup>1</sup>, T. Dahm<sup>2,3</sup>

<sup>1</sup> Universität Leipzig, Institut für Geophysik und Geologie, Leipzig, Deutschland,

<sup>2</sup> Universität Potsdam, Institut für Geowissenschaften, Potsdam, Deutschland,

<sup>3</sup> Deutsches GeoForschungsZentrum, Erdbeben- und Vulkanphysik, Potsdam, Deutschland

Within the ICDP project “Drilling the Eger Rift”, we focus on the German-Czech border region West Bohemia/ Vogtland which is known for its earthquake swarms. These swarms are clusters of small magnitude ( $M_L < 4$ ) earthquakes which are interpreted to be linked to the rise of mostly gaseous fluids with mainly mantle origin. We aim to improve the seismological observation of these small magnitude earthquakes and related processes especially at the upper frequency band of observation by installing three dense small aperture 3D arrays. Each 3D array will consist of a 400 m deep vertical array borehole installation and a small aperture (400 m) surface array.

The drill site S1 in Landwüst and its surroundings serve as pilot site for the first installation. Parallel recordings of borehole and surface stations are available since January 2020, when a borehole chain with eight 3-component 10 Hz geophones was installed. Moreover, we had several surface installations which were equipped with 4.5 Hz 3-component geophones in Spring/Summer 2019 during drilling operations and January 2020 for recording a VSP Experiment. The data were recorded with 400 Hz sampling rate at most locations, but at some selected stations we additionally record data with 1000 Hz sampling rate being the desired sampling rate for the final array configuration. Despite the small aperture of the array, recordings of local earthquakes in June 2019 and January 2020 showed that the amplitude and frequency content of the S-wave and in some cases also the P-wave changes across the array probably caused by the local geology. Due to the high sampling rates and the high frequency content of the recorded earthquake signals, these local site conditions lead to non-coherent waveform recordings for different parts of the array which have a major influence on the overall array performance. However, first tests of broad band frequency wave number analysis (5-180 Hz) in a moving time window (0.2 s) with these data also indicate that the coherency across the array site is still high enough to clearly identify P-waves and S-waves from high-frequency micro-earthquakes.

Furthermore, we evaluate the direct P-wave signal-to-noise ratio (SNR) of more than 200 local earthquakes recorded at the eight borehole stations since January 2020 and report general characteristics of SNR with magnitude, hypocentral distance, and sensor depth, and further the enhanced observable bandwidth of signals. We also use parallel recordings of these borehole stations with 40 4.5 Hz geophones deployed at the surface for an active experiment in January 2020 to estimate signal and noise coherency across the array in different frequency bands for three small magnitude earthquakes and noise during the night. Although the coherence of the earthquake signals decreases by about 40-60% for higher frequencies ( $> 40$  Hz), the recorded noise in the frequency bands above 40 Hz is nearly incoherent across the whole array, therefore the high sampling rates result in a gain in information for the small magnitude earthquakes due to the higher frequency bands.

## Saisonale seismische Aktivität auf dem Mars

M. Knapmeyer, S. C. Stähler, I. Daubar, F. Forget, A. Spiga, T. Pierron, M. van Driel, D. Banfield, E. Hauber, M. Grott, N. Müller, C. Perrin, A. Jacob, A. Lucas, B. Knapmeyer-Endrun, C. Newman, M. P. Panning, R. C. Weber, F. J. Calef, M. Böse, S. Ceylan, C. Charalambous, J. Clinton, D. Giardini, A. Horleston, T. Kawamura, A. Khan, W. T. Pike, J.-R. Scholz, P. Lognonné, B. Banerdt

Die Aktivität der sog. High Frequency Marsbeben (Ereignisse mit einem Frequenzgehalt dominant oberhalb von 2.4 Hz) nahm von Mai bis August 2019 zunächst stark zu, hielt dann (während des Nord-Sommers) auf hohem Niveau an und klang im Frühjahr 2020 fast vollständig ab.

Es ist vorgeschlagen worden (Manga et al., 2019, <https://doi.org/10.1029/2019GL082892>), daß die durch den Mond Phobos verursachten Gezeiten den Porendruck des Grundwassers ausreichend stark verändern könnten, um seismische Aktivität zu induzieren. Ein Spike Train Fourier Spectrum der Ereignisserie zeigt bei den relevanten Perioden (0.31 und 0.43 sols) jedoch keine auffälligen Amplituden. Wir schließen daraus, daß die beobachteten Ereignisse nicht durch Phobos induziert sind.

Wir untersuchen darüber hinaus die Zeitverläufe verschiedener möglicher Ursachen (jahreszeitliche Schwankung der Sonnenhöhe, jährliche solare Gezeiten aufgrund der Bahnelliptizität, jährlicher Zyklus von Verdunstung und Niederschlag von CO<sub>2</sub> an den Polkappen) darauf, wie gut sie den Verlauf der Ereignisrate beschreiben. Eine Maximum-Likelihood-Anpassung entsprechender Rate-Funktionen und ein quantitatives Ranking basierend auf Akaike-Gewichtung und Evidenzgewichten bevorzugt klar die Schwankung der Sonnenhöhe als Ursache, während der CO<sub>2</sub>-Zyklus als am unwahrscheinlichsten bewertet wird. Ein möglicher Mechanismus zur Vermittlung des Sonnenstands in den Untergrund wäre ein Grundwasserabfluß in bekanntermaßen saisonal aktiven Erosionsrinnen, dies ist aber noch genauer zu untersuchen.

Da bislang weniger als ein Marsjahr an Registrierungen vorliegt, kann nicht ausgeschlossen werden, daß es sich nur um eine einmalige Episode handelte. Wir haben daher die verschiedenen Rate-Funktionen in die Zukunft projiziert um abzuschätzen, wann es zu erneuter Aktivität kommen müßte, und wie lange die Phase der relativen Inaktivität dauert.



## A synthetic database of Green's functions and free oscillations for Martian seismology

Sebastian Heimann<sup>1</sup>, Rongjiang Wang<sup>1</sup>, Torsten Dahm<sup>1,3</sup>, Martin Knapmeyer<sup>2</sup>

<sup>1</sup>GFZ German Research Centre for Geosciences, Physics of Earthquakes and Volcanoes, 14473 Potsdam, Germany

<sup>2</sup>Deutsches Zentrum für Luft und Raumfahrt, e.V. (DLR), Institut für Planetenforschung, 12489 Berlin, Germany

<sup>3</sup>Universität Potsdam, Institut für Geowissenschaften, Potsdam, Germany

The InSight (Interior exploration using Seismic Investigations, Geodesy and Heat Transport) mission, which was launched on 5 Mai 2018 and landed on Mars on 26 November 2018, indicated a new epoch of exploration of the red planet. InSight's onboard SEIS (Seismic Experiment for Interior Structure) instrument was deployed to the Mars surface on 19 December 2018. Since then, it has detected more than 450 marsquakes of tectonic origin. For the purposes of Martian seismology, we are going to release a synthetic database of Green's functions (GFDB) and free oscillations based on various seismic reference models of Mars. The GFDB will include full broadband seismograms for the different Mars models, which can be used in combination of the Python toolbox for seismology (Pyrocko) or independently with any other analysis software. A cookbook how to generate own synthetic Green's functions is provided. The database for Mars is prepared as part of a platform which aims to provide elastodynamic Green's functions for different planets and moons. As an example for Martian seismology, we present all free oscillation modes of periods longer than 5 minutes, calculated based on the Mars model DWAK. Particularly we introduce how to determine the eigenfrequencies and quality factors using the code QSSP that is also used to generate the GFDB. The approach used here is independent from the well-known normal-mode approach, but more efficient and accurate than the latter. New suggestions on the synthetic database and its future update will be discussed.



# Data Availability Test for the European Integrated Data Archive using the obspy Routing Client

Stampa, J., Timko, M., Quinteros, J., Meier, T.

September 1, 2020

## Abstract

The European Integrated Data Archive (EIDA) is a distributed federation of datacenters in Europe, dedicated to archiving and providing access to seismic waveform data and metadata. The EIDA-Routing Client from the obspy library in python provides an new and greatly simplified way to request large amounts of data over defined regions and time periods. However, there are problems that frequently arise in downloading, especially of large data sets.

In an effort to provide feedback to the data centers, a coordinated test for the data availability was conducted simultaneously from Christian-Albrechts-Universität (CAU) Kiel, GeoForschungsZentrum (GFZ) Potsdam and Magyar Tudományos Akadémia (MTA) Budapest, repeated once with an interval of 2 weeks.

These tests found some networks completely unavailable through the Routing Client, as well as a surprising variability in the availability of other networks, depending on the time and origin of the request.

## Anwendung des Ausschlusskriteriums Seismische Aktivität bei der Suche und Auswahl eines Standortes für ein Endlager für hochradioaktive Abfälle in Deutschland

Diethelm Kaiser & Thomas Spies

Bundesanstalt für Geowissenschaften und Rohstoffe, Hannover

Im Standortauswahlgesetz § 22 „Ausschlusskriterien“ (2) 4. „Seismische Aktivität“ wird ausgeführt, dass ein Gebiet nicht als Endlagerstandort geeignet ist, wenn die örtliche seismische Gefährdung größer als in Erdbebenzone 1 nach DIN EN 1998-1/NA:2011-01 (DN\_2011) ist. Diese Norm wird in Kürze durch eine Aktualisierung ersetzt, die dem Stand von Wissenschaft und Technik entspricht. Der Entwurf hierzu, E DIN EN 1998-1/NA:2018-10 (DN\_2018), enthält keine Zuordnungen in Erdbebenzonen mehr, sondern weist die seismische Gefährdung räumlich kontinuierlich aus. Dabei beruhen sowohl die Karte der Erdbebenzonen in DN\_2011 als auch die Karte der seismischen Gefährdung in DN\_2018 auf probabilistischen seismischen Gefährdungsanalysen. Die Bundesanstalt für Geowissenschaften und Rohstoffe (BGR) hat im Auftrag der Bundesgesellschaft für Endlagerung mbH einen Vorschlag zur Anwendung dieses Ausschlusskriteriums unter Verwendung von DN\_2018 erarbeitet. Für die Wahl einer Vorgehensweise werden objektive Kriterien aufgestellt und angewendet. Im Ergebnis schlägt BGR vor, als Grenzwert zur Anwendung des Ausschlusskriteriums den Wert im Plateaubereich der spektralen Antwortbeschleunigung von  $1,8 \text{ ms}^{-2}$  in DN\_2018 zu verwenden. Dieser Wert entspricht der makroseismischen Intensität 7, für den die seismische Gefährdung größer als in Erdbebenzone 1 nach DN\_2011 ist. Für solche Gebiete, in denen dieser Wert überschritten wird, gilt das Ausschlusskriterium somit als erfüllt.

Davon unabhängig weisen wir auf ungeklärten Fragen zur Relevanz des Ausschlusskriteriums Seismische Aktivität für die Ermittlung der Erdbebengefährdung eines Endlagers für hochradioaktiver Abfälle hin.

## Dienstag - AK Auswertung

### **Folgen des Grubenwasseranstiegs im östlichen Ruhrgebiet – ein neues Messnetz zur Überwachung der induzierten Mikroseismizität**

Martina Rische, Kasper Fischer, Wolfgang Friederich (Ruhr Universität Bochum)

Im Rahmen des Floodrisk -Projektes (BMBF) werden die Auswirkungen der Anhebung des Grubenwasserspiegels in stillgelegten Bergwerksregionen untersucht.

Aus früheren Studien ist bekannt, dass die Flutung von geschlossenen Bergwerken zum erneuten Anstieg der induzierten Mikroseismizität in diesen Regionen führen kann.

In einem Teilbereich des Projektes soll der Zusammenhang zwischen Grubenwasseranstieg, fluidbedingten Spannungsveränderungen und der induzierten Seismizität im Wasserhaltungsgebiet "Haus Aden" im östlichen Ruhrgebiet näher untersucht werden.

Das seismologische Observatorium der Ruhr Universität baut zu diesem Zweck ein Messnetzwerk bestehend aus ca. 50 seismischen Stationen auf, um die Mikroseismizität flächendeckend überwachen zu können. Bereits im Mai und Juni konnten an 19 Standorten kurzperiodische Seismometer S13 und Mark L4- 3d in Kombination mit EarthData Digitizern installiert werden. Für die Mikroseismizität im Raum Hamm – Bergkamen liegen daher schon erste Ergebnisse vor.

Für die restlichen Standorte sollen Raspberry Shake Sensoren eingesetzt werden, die zur Zeit im Labor konfiguriert und getestet werden.



## Dienstag - AG Seismologie

### **The Slab Puzzle in the Alpine-Mediterranean Region: Insights from a new, High-Resolution, Shear-Wave Velocity Model of the Upper Mantle**

*A. El-Sharkawy<sup>1,2</sup>, T. Meier<sup>1</sup>, S. Lebedev<sup>3</sup>, J. Behrmann<sup>4</sup>, M. Hamada<sup>2</sup>, L. Cristiano<sup>5</sup>, C. Weidle<sup>1</sup>, D. Köhn<sup>1</sup>*

<sup>1</sup> Institute of Geosciences, Christian-Albrechts-Universität, Kiel, Germany

<sup>2</sup> National Research Institute of Astronomy and Geophysics (NRIAG), 11421, Helwan, Cairo, Egypt

<sup>3</sup> School of Cosmic Physics, Geophysics Section, Dublin Institute for Advanced Studies, Dublin, Ireland

<sup>4</sup> Geomar Helmholtz Centre for Ocean Research, Kiel, Germany

<sup>5</sup> Deutsches GeoForschungsZentrum (GFZ), Telegrafenberg 14473, Potsdam, Germany

The fascinating complexity of the Mediterranean caused by small, strongly-curved retreating subduction zones and associated back-arc basins as well as continental collision along the northern and eastern margins of the Adriatic microplate is driven by strongly fragmented subducting slab segments. It remains however a challenge to resolve their geometry in the Mediterranean upper mantle. We present a new shear-wave velocity model of the Mediterranean upper mantle (MeRE2020) down to 300 km depth, constrained by a very large set of over 200,000 broadband (8 - 350 s), inter-station, Rayleigh wave, phase velocity curves, that illuminates the complex structure and the highly fragmented nature of the subducting slabs in the Mediterranean upper mantle. Phase-velocity maps computed using these measurements were inverted for depth-dependent, shear-wave velocities using a new implementation of the stochastic particle-swarm-optimization algorithm (PSO). The resulting 3-D model makes possible an inventory of slab segments across the Mediterranean. Fourteen slab segments of ~200 - ~800 km length along-strike are identified. The location of slab segments are consistent with and validated by the intermediate-depth seismicity, where it is present. We distinguish attached slab segments reaching down to the bottom of the model from shallow slabs that terminate at shallower depths and from detached ones that are not connected to the lithosphere in the foreland. The new high-resolution tomography demonstrates the intricate relationships between slab fragmentation and the evolution of the relatively small and highly curved subduction zones and collisional orogens characteristic of the Mediterranean realm but also the need for further imaging of the detailed 3D geometry of the slab segments.

## **Imaging Seismic Wave-Fields with AlpArray and Neighboring European Networks**

M. Tesch, J. Stampa, T. Meier

The modern-day coverage and availability of broad-band stations in the greater Alpine area offered by AlpArray, Swath-D and the European seismological networks allows for imaging seismic wave-fields at yet unprecedented resolution. In the AlpArray area and in Italy, the distance of any point to the nearest station is less than 30km, resulting in an average inter-station distance of about 45km. With a much denser deployment in a smaller region of the Alps (320km in length and 140km wide), the Swath-D network possesses an average inter-station distance of about 15km.

We show single event seismogram sections, time slices of teleseismic and regional wave-fields, and wave-field animations to reveal both the resolution capabilities of this dense station distribution as well as the enormous spatio-temporal complexity of seismic wave propagation. The time slices and wave-field animations demonstrate the need for dense regional arrays of broad-band stations, such as provided by AlpArray and neighboring networks, to resolve properties of teleseismic wave-fields. Here we present the images of coherent arrivals of direct body and surface waves, multiple body wave reflections, and multi-orbit phases for teleseismic events.

Spatial observations of the wave-fields illustrate e.g. the decrease in horizontal wavelength from P to S to surface waves and the way in which they considerably deviate from plane waves, due to heterogeneous earth structures along the path from the source to the array and beneath the regional array itself. Tomographic imaging techniques for the deep structure beneath the regional array have to take this spatio-temporal variability into account and correct for it.

The lateral resolution of the regional broad-band array is however dependent on station density, in this case limited to about 100km. Only even denser station distributions like those provided by Swath-D suffice to recover wave-fields of short period body and surface waves.

## **Focal mechanisms for small to intermediate earthquakes in the northern part of the Alps and estimations of the regional crustal stress field**

**Thomas Plenefisch<sup>1</sup>**, Laura Barth<sup>1</sup>, Mathias Hoffmann<sup>1</sup>, Christian Brandes<sup>2</sup> and the AlpArray working group\*

- <sup>1</sup>Federal Institute for Geosciences and Natural Resources, B4.3, Hannover, Germany ([thomas.plenefisch@bgr.de](mailto:thomas.plenefisch@bgr.de))
- <sup>2</sup>[Leibniz Universität Hannover](http://www.geologie.uni-hannover.de), Institut für Geologie, Hannover, Germany

In the multinational AlpArray project over 600 seismic broadband stations have been installed and operated in the broader Alpine region over the last years. Supplemented by the existing permanent stations in the area it is one of the most densely spaced seismic networks worldwide. The huge amount of stations offers an excellent opportunity to study crustal seismicity and to calculate focal mechanisms even for small magnitude earthquakes with high accuracy.

In our study we focus on small to intermediate earthquakes that occurred in the area of the Northern Alpine chain. The events are roughly clustered in four distinct sub-regions. From West



to East these are (1) the Lake Constance area (2) the Arlberg region (3) the area of Garmisch-Partenkirchen and (4) the broader region of Innsbruck. We calculated the focal mechanisms using the FOCMEC program (Snoko, 2003) and used polarities of P waves as well as amplitude ratios of SH to P as input parameters in the inversions.

Altogether, we calculated focal mechanisms for 20 earthquakes in the magnitude range between 2.5 and 3.5 from the time period 2016 to 2020. The focal mechanisms are of diverse faulting type. They preferably show reverse or strike-slip faulting, normal faulting events are rather the exception. We analyse the mechanisms with respect to lateral changes along the Northern Alpine chain and compare them to moment tensors of events of slightly larger magnitudes (Petersen et al., 2019). Furthermore, we compare our mechanisms to the orientations of faults and use the focal mechanisms as input to invert for the stress field.

### **Analysis of the seismicity and stress field of the Albstadt Shear Zone, Germany**

Mader, S.<sup>1</sup>, Reicherter, K.<sup>2</sup>, Ritter, J.<sup>1</sup> and the AlpArray Working Group

<sup>1</sup>KIT, Geophysical Institute, Karlsruhe, Germany

<sup>2</sup>RWTH Aachen, Neotectonics and Natural Hazards, Germany

In the last century alone three earthquakes with ML greater five occurred on the Swabian Alb close to the town Albstadt, SW Germany. The earthquakes rupture the approx. 20-30 km long, N-S striking left-lateral strike slip fault zone, called the Albstadt Shear Zone (ASZ). This fault zone can only be studied by its seismicity as there is no surficial expression of the ASZ.

We use the earthquake catalog of the State Earthquake Service of Baden-Württemberg from 2011 to 2018 and complemented it with additional phase picks on four AlpArray seismic stations as well as five additionally installed seismic stations of the Karlsruhe BroadBand Array. We used the best subset of this catalog to invert for a new minimum 1D seismic velocity model of our study area. Next, we relocated the whole catalog and calculated fault plane solutions from which we estimated the direction of the maximum horizontal stress field.

The velocity model reveals a simple structure for the area around the ASZ. The corresponding station corrections show a simple pattern, which we explain by the depth variations of the crystalline basement. The seismicity aligns north-south and is concentrated between the towns Tübingen und Albstadt around the 9°E meridian and covers a depth range of 1.5 to 16 km. We can identify different clusters of events hinting a segmentation of the ASZ. The dominating focal mechanism is strike-slip, but we also observe minor components of normal and reverse faulting. The derived corresponding direction of the maximum horizontal stress field is 147°, which is similar to prior studies.

Our results image the ASZ by its mainly micro-seismic activity between 2011 and 2018 confirming the N-S striking character, but also indicating a more complex fault system.

We thank the State Earthquake Service in Freiburg for using their data (Az. 4784//18\_3303).

## **Large temporal and short spatial scales – two microseism observations in the North and Baltic Seas**

Becker, D.<sup>1</sup>, May, T.<sup>2</sup>, Dethof, F.<sup>1,3</sup>, Meier, T.<sup>2</sup>

<sup>1</sup>Universität Hamburg, Institut für Geophysik, Hamburg

<sup>2</sup>Christian-Albrechts-Universität Kiel, Institut für Geowissenschaften, Kiel

<sup>3</sup>now at: Helmut-Schmidt-Universität Hamburg, Hamburg

When studying ocean microseism, two of the most interesting questions are: a) How does the generation of ocean microseism change with long term changes of weather patterns and is it possible to use the recordings of ocean microseism as proxy data for long term climate changes? b) Where exactly is (local) ocean microseism generated? We present some observations from the North and Baltic Seas that compare the local microseism (with frequencies > 0.2Hz) with the index of the North Atlantic Oscillation (NAO) which governs the characteristics of storm systems in the North Atlantic and adjacent marginal seas. While it is difficult to identify correlations on short time scales of days or weeks, low pass filtered time series of microseism energy profiles and the NAO index exhibit a positive correlation.

While most of the local microseism energy generation is governed by wind generated ocean waves, an influence of the tidal dynamics on the generation of local microseism was found for the area around Helgoland in former studies. Here, we present results from beamforming analysis for a small aperture array (HelgA array) installed on the island of Helgoland to gain insight into the source regions of this tide-influenced microseism. We observe indications for different source regions during rising and falling. These different regions might be linked to the strengths of tidal currents during the progression of the tidal signal along the German Bight.

## **Microseismicity indicates a current transition from rifting to spreading at the southern Fonualei Rift and Spreading Center in the Lau Basin**

Florian Schmid, Max Cremanns, Nico Augustin, Dietrich Lange, Florian Petersen, Heidrun Kopp

GEOMAR Helmholtz Zentrum für Ozeanforschung Kiel

Young extension centers in the proximity of back-rolling subduction zones constitute an ideal natural laboratory to investigate the early evolutionary stages of back-arc basins. We present a catalog of 711 microearthquakes recorded during a 32-days deployment of ocean bottom seismometers at the southern part of the Fonualei Rift and Spreading Center in the Lau Basin. The majority of epicenters are concentrated along the central region of the axial valley and about 450 events are associated with an earthquake swarm that is likely linked to magmatic diking in the crust. The earthquake swarm location coincides with several volcanic mounds on the seafloor, covered by fresh lava flows. The spatial distribution of microearthquakes and the maximum depth of brittle faulting is more similar to oceanic spreading centers than to continental rift zones. We interpret our results in conjunction with refraction seismic data and magnetic anomaly data from the same region. In combining all findings, we conclude that the southern Fonualei Rift and Spreading Center is currently in transition from a rifting dominated mode of extension to a seafloor spreading dominated mode of extension. This transition may be associated with fundamental changes in the underlying mechanisms of melt generation leading to a diminishing influence of hydrous flux melting and the growing influence of decompression melting at this back-arc extension zone.



## **Global seismic ambient noise reduction due to COVID-19 pandemic lockdown measures**

S. Donner <sup>1</sup>, K. Stammer <sup>1</sup>, T. Megies <sup>2</sup>, and J. Wassermann <sup>2</sup>;  
based on Lecocq et al. (76 co-authors)

1. Federal Institute for Geosciences and Natural Resources (BGR), Hannover, Germany
2. Department of Earth Sciences, LMU München, Germany

It is well known that human activity is contributing strongly to the seismic ambient noise field in higher frequencies. The overall amount can be determined roughly from the reduced noise level during the generally very quiet Christmas/New Year season. However, a detailed understanding of the human contribution is missing so far. The globally extensive pandemic lockdown measures provide a unique chance to better characterise the man-made part of the ambient seismic noise field. Never before a period of quiescent have been lasting for so long and with such a strong reduction in amplitude and on a global scale.

In a unique effort Thomas Lecocq from Royal Observatory of Belgium gathered more than 70 scientists from 66 institutes and 27 countries via social media. Jointly, we collected data from 268 stations and could show that 185 of them in 77 countries show clear reduction effects. This study is recently published in a Science article. The amplitude reduction of the seismic ambient noise reached up to 50%. Even in Germany, where lockdown measures have been rather moderate, some stations show a clear reduction of the ambient noise between 25% (GR.BFO) and 60% (BW.ZUGS).

Here, we present the main conclusions of the paper and, thus, providing several starting points for future research. These very first findings from the quiescent period resulted in the announcement of a special issue on this topic in EGU's Open Access Solid Earth journal (submission deadline end of November 2020).

Title: An Ambient Noise and Receiver Function Study of the Oman Ophiolite and the Lithosphere of the Eastern Arabian Continental Margin

Authors: Lars Wiesenberg<sup>1</sup>, Christian Weidle<sup>1</sup>, Amr El-Sharkawy<sup>1,2</sup>, Philippe Agard<sup>3</sup>, Andreas Scharf<sup>4</sup>, Frank Krüger<sup>5</sup>, Thomas Meier<sup>1</sup>

Affiliation: Institute of Geosciences, Christian-Albrechts-University Kiel<sup>1</sup>; National Research Institute of Astronomy and Geophysics, Cairo, Egypt<sup>2</sup>; University Pierre et Marie Curie Paris, France<sup>3</sup>; Sultan Qaboos University Muscat, Oman<sup>4</sup>; Institute of Earth and Environmental Sciences, University Potsdam<sup>5</sup>

The lithospheric structure of the northern Oman continental margin – covered by the Oman ophiolite, the world's reference example of obducted oceanic lithosphere – has so far been imaged by only a few, local 2D active seismic and gravity studies. Little is known about the physical properties of the Arabian continental lithosphere in the area of the Oman Mountains and the Batain area in the SE. The northern and eastern coasts in the Oman have been passive margins since the Permo-Triassic. In the late Cretaceous, retreating subduction led to ophiolite obduction. Since then, the northeastern Arabian margin has been subjected to post-obductional extension and subsequent formation of the northern Oman Mountains around 30 Ma ago, leaving the ophiolite resting on their flanks.

To image the lithosphere structure in the area, a temporary broadband seismic network with 40 instruments for continuous recording has been operated for 2 years from October 2013 to February 2016. The dataset is complemented by data of 18 permanent broadband seismometers, operated by the Earthquake Monitoring Centre Oman, the Dubai Seismic Network and the Global Seismographic Network. Here, a 3D shear-wave velocity model of the lithosphere beneath the eastern Arabian continental margin is presented by using ambient seismic noise tomography. A newly implemented approach for automated inter-station phase velocity measurements based on the fitting of the phase of the Bessel function of third kind to the phase of the ambient noise correlations was applied to compute Rayleigh and Love wave fundamental mode phase velocities in a period range of 2 – 40 s. Rayleigh and Love wave phase velocity maps are calculated, which show velocity anomalies across the eastern Arabian continental margin as a function of period. We then simultaneously inverted Rayleigh and Love wave local dispersion curves for shear wave velocity over depth by using a novel implementation of a radially anisotropic, probabilistic 1D inversion (Particle Swarm Optimization). By introducing radial anisotropy to the inversion scheme, the results improve significantly compared to an isotropic inversion of Rayleigh and Love wave dispersion curves. The resulting 1D models are combined to construct the 3D model of isotropic shear wave velocity and radial anisotropy to a depth of 55 km beneath the eastern Arabian continental margin. First order interpretation will be discussed, including distinct differences in the upper crustal structure below the Oman Mountains and the undeformed Arabian platform further south. The crustal thickness changes in their architecture with an overall thinning towards the east and a local thickening below the mountain range. Receiver Functions are added to map deeper structural discontinuities in the lithosphere below the study area.



# Seismizität und Spannungszustand im Omangebirge

Elisabeth Glück, Christian Weidle, Thomas Meier

Am östlichen Kontinentalrand der arabischen Platte befindet sich die Al-Hajar Gebirgskette mit einer Topographie von bis zu 3000m, welche ab dem Oligozän in die heutige Form herausgehoben wurde. Das Gebirge ist zu weiten Teilen von dem bekannten Oman Ophioliten bedeckt, dem größten zusammenhängenden Fragment ozeanischer Lithosphäre an Land.

Auf der eigentlich als seismisch inaktiv geltenden Arabischen Platte wurden in der Vergangenheit im Bereich des Oman Gebirges durchaus, vorwiegend kleinere Erdbeben registriert. Somit stellt sich die Frage nach der Seismizität im Omangebirge und dem damit zusammenhängenden Spannungszustand in dieser Region. Hierfür wurden erstmals die Daten eines dichten temporären Seismometernetzes ausgewertet und mit den Daten des permanenten seismischen Netzes im Oman verglichen.

Zunächst konnten Lokalisierungen zwischen dem permanenten und dem dichten temporären Netz abgeglichen werden. Es zeigt sich, dass das permanente Netz seismische Ereignisse im Oman Gebirge hinreichend gut erfasst und lokalisiert, so dass der seit 2003 bestehende Erdbebenkatalog eine zuverlässige Quelle darstellt.

Um die Seismizität im Omangebirge besser zu verstehen, wurden zu den zwischen 2013 und 2016 am temporären Netz lokalisierten und als tektonisch eingestuft Ereignissen erstmals für die Region Herdflächenmechanismen anhand der Polaritäten der P-Wellen Ersteinsätze bestimmt. Die Momentenmagnituden der Beben lagen zwischen 1,7 und 3,3. Während der Laufzeit des Projekts wurden 15 Ereignisse als tektonisch eingestuft.

Vor allem im Bereich des Semail Gap und der Wadi Mansah Fault Zone zeigen diese vorwiegend Transtension, während im Norden auf der Musandam-Halbinsel vorwiegend Transpression vorherrscht.

Des Weiteren wurde eine Spannungsinversion für die als tektonisch eingestuften Events durchgeführt. Diese ist trotz der geringen Anzahl an Events recht stabil und zeigt vor allem, dass die Hauptspannungsrichtung von Nordost nach Südwest gerichtet ist.

Im Norden dominiert somit möglicherweise der Einfluss der kontinentalen Kollision zwischen Arabien und Eurasien das Spannungsfeld. Im zentralen und östlichen Bereich des Omangebirges scheinen die maximale Horizontal- und die Vertikalspannung annähernd gleichgewichtet. Der Einfluss der Makran-Subduktionszone auf das Spannungsfeld lässt sich nur schwer quantifizieren, aber Beiträge zum Spannungsfeld von Extension durch slab-pull oder die Bildung eines forebulges im Bereich des Oman-Gebirges sind vorstellbar.



# Mittwoch - AG Seismologie

Borns, J., U. Wegler  
Friedrich-Schiller Universität Jena

Abstract: „Analyse der P- und S-Wellen-Dämpfung der oberflächennahen Schichten im Oberrheingraben mittels Bohrlochseismometern“

Im Rahmen des Verbundvorhaben SEIGER: „Monitoring tiefer Geothermischer Anlagen und mögliche seismische Einwirkungen“ wurden die oberflächennahen Dämpfungseigenschaften im Oberrheingraben mit Hilfe von Bohrlochseismometern untersucht. Es wurden für 59 lokal registrierte induzierte Erdbeben die Seismogramme an 4 Bohrlochseismometer (Teufe 70 – 305 m) untersucht. Stärkere Ausschläge kurz nach dem Ersteinsatz von sowohl P- als auch S-Wellen werden als Reflexionen dieser Wellen an der freien Oberfläche angesehen. Das hieraus resultierende Spektralverhältnis dient zur Ermittlung der oberflächennahen frequenzabhängigen Dämpfung ( $Q^{-1}$ ). Für die bisher am detailliertesten analysierte(?) Station ROTT mit einer Teufe von 305 m ergeben sich daraus für einen Frequenzbereich von 10 -100 Hz ein  $Q^{-1}_p$  von 10 -140 und für  $Q^{-1}_s$  ein Bereich von 7-135. Im Allgemeinen erhöht sich die Dämpfung mit steigender Frequenz. Bei Anwendung des Potenzgesetzes  $Q(f)^{-1} = Q^{-1}_0 * f^m$ , ergibt sich anhand einer Regressionsanalyse folgende Beziehung:  $\log_{10}(Q^{-1}_p) = -1.06 * \log_{10}(f) - 0.93$  und  $\log_{10}(Q^{-1}_s) = -1.1 * \log_{10}(f) - 0.87$ . Das größte Problem bei dieser Analyse stellen Coda/Streu-Wellen dar, die den direkten P- und S-Wellen folgen, und damit in einem ähnlichen Zeitfenster wie die an der Oberfläche reflektierten Wellen registriert werden.

## Shear wave velocity from inter-source interferometry: Application to 2018 West Bohemia earthquake swarm

Tom Eulenfeld

Institut für Geowissenschaften, Friedrich-Schiller-Universität Jena

The concept of seismic interferometry embraces the construction of waves traveling between receivers or sources with cross-correlation techniques. Here, I use the the time lag of the maxima in the cross-correlation of the coda wave field to measure the shear wave velocity in the source volume of swarm earthquakes. This technique is different from previous studies analyzing the decorrelation of the coda wave field of nearby events or using the cross-correlation for relocation purposes.

The technique is applied to five event clusters of the 2018 West Bohemia earthquake swarm. With the help of a high quality earthquake catalog, I was able to determine the shear wave velocity in the region of the five clusters separately. The shear wave velocities range between 3.5 km/s and 4.2 km/s. The resolution of this novel method is given by the extent of the clusters and better than for a comparable classical tomography. The method can be incorporated into a tomographic inversion to map the shear wave velocity in the source region with unprecedented resolution. The influence of focal mechanisms and the attenuation properties on the polarity and location of the maxima in the cross-correlation functions is discussed.

## Scherwellen-Doppelbrechung von SK(K)S-Phasen und lateral variierende Anisotropie im Gebiet des Oberrheingrabens

Yvonne Fröhlich, Michael Grund und Joachim R. R. Ritter

Geophysikalisches Institut (GPI), Karlsruher Institut für Technologie (KIT), Karlsruhe, Deutschland

Vorliegende S-Wellen-Splitting-Messungen (SWSM) an Phasen vom SKS-Typ im Gebiet des Oberrheingrabens (ORG) weisen eine Variation der bestimmten (scheinbaren) Splitting-Parameter sowie der Null- und Nicht-Null-Messungen mit dem Rückazimut auf und zeigen darüber komplexe, eingeschlossen lateral variierende, Anisotropie an. Durch diese Beobachtung motiviert, das Modell der Anisotropie im Gebiet des ORGs zu verbessern, wurden weitere SWSMen an Langzeitregistrierungen an breitbandigen seismischen Messstationen durchgeführt.

Hinsichtlich der Anisotropie im Mantel wurden PKS-, SKS, und SKKS-Phasen teleseismischer Erdbeben innerhalb des Epizentraldistanz-Bereichs  $[90,140]^\circ$  herangezogen. Die Splitting-Parameter, die schnelle Polarisationsrichtung  $\phi$  angegeben als Winkel zu Nord und die Verzögerungszeit  $\delta t$  akkumuliert zwischen den beiden quasi S-Wellen, wurden mit dem *MATLAB*-Programm *SplitLab* zusammen mit der Erweiterung *StackSplit* bestimmt. Es wurden als Grenzfrequenzen für den Bandpass-Filter  $[0.020,0.066]$  Hz (untere Grenze) und  $[0.15,0.20]$  Hz (obere Grenze) gewählt und die *Energie-Minimum-Methode* und die *Rotation-Korrelation-Methode* vergleichend angewendet. An die bestimmten (scheinbaren) Splitting-Parameter der Nicht-Null-Messungen wurden strukturelle Anisotropie-Modelle zu den Modelltypen eine Schicht und zwei Schichten mit transversaler Isotropie mit horizontaler und geneigter Symmetrieachse angepasst.

Die stationsbezogenen Resultate wurden stationsübergreifend hinsichtlich möglicher grundlegender Anisotropie-Regime betrachtet. Entsprechend der Länge der Verzögerungszeit liegt die Anisotropie im oberen Mantel (Lithosphäre und Asthenosphäre). Verifiziert werden konnte, dass die Anisotropie im Gebiet des ORGs nicht nur vertikal, sondern auch kleinräumig lateral variiert.



## KNIPAS Projekt: Analyse der oberen Mantelstrukturen entlang des ultra-langsam spreizenden Knipovich Rückens

T. Rein<sup>1</sup>, F. Krüger<sup>1</sup>, V. Schlindwein<sup>2</sup>

<sup>1</sup> Institut für Geowissenschaften, Universität Potsdam, Karl-Liebknecht Str. 24-25, D-14476 Potsdam-Golm

<sup>2</sup> Alfred Wegener Institut, Am Alten Hafen 26, D-27568 Bremerhaven

Der Knipovich Rücken ist ein ultra-langsam spreizender Mittelozeanischer Rücken und liegt in der Grönlandsee südwestlich von Spitzbergen. Ultra-langsam spreizende Mittelozeanische Rücken haben eine Spreizungsrate von weniger als 20 mm/a und unterscheiden sich zudem in der Schmelzproduktion, Krustenmächtigkeit und Seismizität stark von schnell spreizenden Rücken. Charakteristisch für ultra-langsam spreizende Rücken sind massive Vulkankomplexe, die bis zu 100 km voneinander entfernt liegen und von amagmatischen Bereichen getrennt werden. Im Gegensatz zu den schnell spreizenden Rücken findet die Schmelzzufuhr bei den ultra-langsam spreizenden Rücken überwiegend an den Vulkanen statt. Folglich variiert die Krustenmächtigkeit entlang des Rückens stark. Während die Krustenmächtigkeit an den Vulkanen besonders dick ist, ist die Schmelzzufuhr in den amagmatischen Bereichen so gering, dass dort Mantelgestein an der Oberfläche exponiert ist. Auffallend sind zudem Lücken in der Seismizität, die innerhalb der amagmatischen Segmente in den oberen 10 km beobachtet wurden und mit einem hochgradig serpentinisiertem Material in Verbindung gebracht werden.

Das KNIPAS (Knipovich Ridge passive seismic experiment) Projekt befasst sich mit den aktiven Spreizungsprozessen entlang ultra-langsam spreizender Rücken. Um diese Prozesse besser verstehen zu können, werden die Seismizität und die Struktur des oberen Mantels erstmals entlang eines ganzen Segmentes des Knipovich Rückens untersucht. Im Zuge dessen ist zwischen Juli 2016 und Oktober 2017 ein seismisches Array, bestehend aus 30 Ozeanbodenseismometern installiert worden. Das seismische Array um den Logachev Seamount erstreckt sich über eine Länge von 160 km. Die Daten wurden durchgehend mit einer Abtastrate von 50 Hz, bzw. 100 Hz (rund um Logachev Seamount) aufgezeichnet.

Ziel dieses Teilprojektes ist die Charakterisierung der Struktur des oberen Mantels mithilfe von Oberflächen- und teleseismischer Raumwellen. Eine erste Auswertung der Kreuzkorrelationen des seismischen Hintergrundrauschens der vertikalen Komponenten deutet auf einen Frequenzgehalt von 3-10 s und Rayleighwellen-Geschwindigkeiten zwischen 800-950 m/s hin. Außerdem lässt sich eine Veränderung des seismischen Hintergrundrauschens mit den Jahreszeiten beobachten.



## Donnerstag - AG Seismologie

### **The 1995 Mw 7.2 Gulf of Aqaba Earthquake revisited: estimating the fault geometry and rupture evolution from geodetic and teleseismic data**

Vasyura-Bathke<sup>1</sup>, Hannes; Steinberg<sup>2</sup>, Andreas; Krüger<sup>1</sup>, Frank; Jónsson<sup>3</sup>, Sigurjón; Mai<sup>3</sup>, Paul Martin; Feng<sup>4</sup>, Guangcai;

1- University Potsdam, Potsdam, Germany

2- Bundesanstalt für Geowissenschaften und Rohstoffe BGR, Hannover, Germany

3- King Abdullah University of Science and Technology, Thuwal, Saudi Arabia

4- Central South University, Changsha, China

The largest earthquakes in Saudi Arabia occur at the northwestern boundary of the Arabian plate on a system of left-lateral transform faults extending from the Red Sea in the South and North through the Gulf of Aqaba. The last major earthquake along this boundary occurred in November 1995 and was located offshore within the central-north part of the gulf, where the complex fault system consists of several transform faults and pull-apart basins. Various researchers studied the source parameters of this earthquake in the past, either by using geodetic radar (InSAR) or teleseismic (P and S waves) data, and several source models of the earthquake rupture and the active fault segments were proposed. However, these source models differ significantly from each other and it still remains unclear which fault segments within the Gulf were activated during the event.

In this work, we use results from multi-array teleseismic back-projection and the surface trace of the main fault rupture as mapped from the GAST-project multibeam bathymetric survey data to pre-define the location of the main fault segments. With both the geodetic data (InSAR and radar-image offset data) and the teleseismic data we then estimate the segment geometries and rupture evolution in a joint Bayesian estimation.

Our results show that neither dataset alone can properly constrain the parameters of the activated faults within the gulf. However, the combination of these data sets shows consistent features allowing to draw a clearer picture of the rupture evolution of the earthquake.

### **Seismic imaging of magmatic systems: from rock to mantle.**

Luca de Siena

Johannes Gutenberg University Mainz

Modelling structure and dynamics of magmatic systems requires an integration of interdisciplinary techniques, which are applied when either unrest at a monitored volcano starts or there are signals of volcano reawakening. What these techniques heavily rely on for their interpretation are seismic tomography models that are increasingly based on the use of full waveform information. To date, despite the availability of massive active seismic datasets, we still lack a proper full-waveform tomography model analogue to those available in exploration seismology. The main reason is the intrinsic heterogeneity of volcanic media, especially that of their shallowest layers and geomorphology, generating signals corrupting

any standard seismic imaging technique. Here, I will discuss research focused on including recent advances in modelling of amplitude and phases in highly-heterogeneous structures into a proper tomographic framework, with in mind the needs of the community modelling volcano dynamics. This research tackles seismic imaging from the rock up a wider range of field scales. While it is today acknowledged that stochastic information can be used to better image volcanic structure, we can do more: (1) linking continental-scale seismic imaging with local volcano tomography models; (2) modelling which petro-mineralogical parameters control seismic phases and amplitudes in volcanic rock samples; (3) recognising the importance of setting anisotropic and viscous matrices in the forward modelling of seismic wave propagation. These efforts will eventually build better, quantitative foundations to the bridge connecting seismic imaging with volcanology.

### **A self-similar rupture model for efficient teleseismic source modeling**

T. Dahm<sup>1,3</sup>, S. Heimann<sup>1</sup>, M. Metz<sup>3</sup>, M. Isken<sup>2</sup>

<sup>1</sup>GFZ German Research Centre for Geosciences, Physics of Earthquakes and Volcanoes, Potsdam, Germany

<sup>2</sup>Universität Kiel (CAU), Geowissenschaften, Kiel, Deutschland

<sup>3</sup>Universität Potsdam, Institut für Geowissenschaften, Potsdam, Deutschland

Retrieving the space-time history of earthquake rupture in a robust and systematic manner, and if possible within short time after the earthquake, is a key question in seismology and important for seismic hazard, early warning and damage assessments. We develop a flexible, physics-based rupture model depending on few parameters only, so that non-uniqueness is reduced and the uncertainty estimation is feasible in near-real time.

Rupture is simulated on a regular grid on an arbitrary oriented, curved plane. A single nucleation point is considered, and the spreading rupture front is approximated by iteratively solving the Eikonal equation with a space dependent rupture velocity. For the sake of simplicity, the rupture velocity scales with the shear wave velocity. Instead of applying smoothness constraints for slip, we impose a spatially variable stress-drop and calculate the time-dependent, quasi-static slip at each grid point by means of a boundary element method, using the instantaneous rupture front to define the shape of the crack at each time step. A source time function is implicitly derived at each spatial grid point.

If shear wave velocities and shear stress (drop) are given as background models for the region under study, the model has only three additional free parameter in comparison to the point source moment tensor model, i.e. the nucleation point and a scaling factor of the rupture velocity. We introduce the basic concepts of the self similar rupture model and discuss examples of rupture simulations. The new model will be integrated in *Pyrocko*, a Python toolbox for seismology.

## **Strong topography of the mid-mantle reflector beneath the Northern Atlantic**

Morvarid Saki <sup>a</sup>, Christine Thomas <sup>a</sup>, Rafael Abreu <sup>a</sup>

<sup>a</sup> Institute of Geophysics, University of Münster, Münster, Germany

We investigate the seismic structure of the mid-mantle beneath the North Atlantic using PP and SS underside reflections off a potential mid-mantle reflector. We analyzed over 2600 seismograms from earthquakes with  $M_w \geq 5.8$  using array seismic methods to improve the visibility of the reflected signals. The measured time lag between PP/SS arrivals and their corresponding precursors on robust stacks are used to estimate the depth of the reflector. Our results reveal the presence of mid-mantle reflectors beneath the North Atlantic within the depth range of ~700 to 1300 km which are consistent for both P and S wave observations. The reflectors' depths show a variation of shallower than 1000 km beneath the southern part of the investigation area to deeper values towards the northern part of the North Atlantic. Measuring the polarity and amplitudes of mid-mantle reflected waves with respect to the main phase indicates a velocity increase over the reflector for most cases. The area where the reflector changes depth generates variations in the waveforms, which we confirm by 3D waveform modelling.

## **A new look at Polarities of D'' reflections - implications for mineralogy**

Christine Thomas<sup>a</sup>, Laura J. Cobden<sup>b</sup>, Art R.T. Jonkers<sup>a</sup>

<sup>a</sup> Institute of Geophysics, University of Münster, Münster, Germany

<sup>b</sup> University Utrecht, The Netherlands

Polarities of seismic reflection of P and S-waves at the discontinuity at the top of D'' are usually assumed to indicate the sign of the velocity contrast across the D'' reflector. For reflections in paleo-subduction regions the S-wave reflections off D'' (SdS) are the same as ScS and S, indicating a positive velocity contrast at the reflector. In recent years, an opposite polarity of PdP waves (P-reflection at the D'' discontinuity) has been observed in some regions, partly dependent on travel direction, partly dependent on distance. This would indicate a velocity reduction in P-waves where a velocity increase is detected in S-waves. This phenomenon can be explained with the presence of post-perovskite below the top of D'', but azimuthal dependence of PdP polarities can be better explained with anisotropy. Here we re-analyse PdP and SdS wave polarities and, when modelling the polarities and amplitudes using Zoeppritz equations, we find that a ratio of  $dV_s/dV_p = R$  of larger than 3 reverses polarities of P-waves in the absence of anisotropy, i.e. we find a polarity of PdP that might be interpreted as a velocity decrease but could actually represent a velocity increase. The S-polarity stays the same as S and ScS and does not change even with large R. Observed values of R above 4 have been reported recently, so these cases do exist in the lower mantle. Using a set of 1 million models with varying minerals and processes across the boundary, we carry out a statistical analysis (Linear Discriminant Analysis) and find that there is a marked difference in mantle mineralogy to explain R values larger and smaller than 3, respectively. The regime of cases with R-value larger than 3 for both velocity increases is mostly due to an increase in MgO/FeO and post-perovskite across the discontinuity. In regions where both velocities are negative, a decrease of FeO and MgO can explain the R values. In regions where high R is observed, alternate explanations of lowermost mantle composition versus anisotropy can then be tested by measuring polarities in different azimuths.



# ”Two double couple synthetic waveforms inversion”

A. Carrillo Ponce<sup>1</sup>, T. Dahm<sup>1</sup>, S. Cesca<sup>1</sup>, F. Tilmann<sup>1</sup>, A. Babeyko<sup>1</sup>, S. Heimann<sup>1</sup>

<sup>1</sup>*Helmholtz-Zentrum Potsdam Deutsches GeoForschungsZentrum, Potsdam, Germany*

E-mail address: carrillo@gfz-potsdam.de

## Abstract

Rupture modeling is the first phase of the PhD project ”Effect of multi-fault ruptures for tsunami hazard estimation” which aims to analyse tsunami potential produced from complex ruptures geometries in order to improve tsunami hazard maps and early warning. The quantification of the role of rupture complexity in ground shaking and surface slip is however the first step. From literature we select 5 events (Samoa 2009, Haiti 2010, Sumatra 2012, Kaikoura 2016 and Alaska 2018) that present characteristics of multiple faults in the main rupture and a big CLVD component. As all these events are big enough ( $M_w \geq 7.0$ ) and shallow ( $< 50$  km), moment tensor inversions are run using teleseismic body waves data (P and S phases).

When multiple ruptures contribute to the total energy release, the wavefield is a superposition of the individual signals, even if the individual mechanisms are spatially or temporally separated, which makes it very difficult to identify subevents. As a first step synthetic waveforms are generated in order to analyse and quantify the impact of subevents in multiple source moment tensor inversion.

We generate a synthetic earthquake free of noise triggered by two double couple sources with strike-slip mechanisms (which follow a similar geometry as Alaska 2018 earthquake, one of the database events) to analyse the moment tensor inversion results as we change the time difference, distance, relative strength and depth between both sources. To make the separation of the two sources clear, the synthetic rupture is composed by two sources separated in time by 60 s, both at 10 km of depth, at a distance of 5 km between them, with same relative strength and an azimuth of  $0^\circ$ . In order to analyse the effect of the mechanism in the inversion results, we perform this test twice. The first test includes a synthetic earthquake composed by two sources with the same mechanism (left lateral strike-slip) and the second test includes an earthquake composed by two sources with different mechanisms (left lateral and right lateral strike-slip). The forward modeling shows the changes in waveforms for each parameter according to the configuration and the principal change when including different mechanisms in the rupture is the amplitude of the first source. The simultaneous inversion for two point sources is very stable (low standard deviations) and mean solutions for every parameter remains close to the reference value.

# Donnerstag - AK Wind

## Seismic signals from wind turbines – amplitude decay from long-term observations and modeling of seismic radiation

M. Lindenfeld<sup>1</sup>, F. Limberger<sup>1,2</sup>, G. Rumpker<sup>1</sup> and H. Deckert<sup>2</sup>

<sup>1</sup>Institute of Geosciences, Goethe-University Frankfurt, Frankfurt am Main, Germany (lindenfeld@geophysik.uni-frankfurt.de)

<sup>2</sup>Institute for Geothermal Resource Management, Mainz, Germany, (limberger@igem-energie.de)

As part of the KWISS-project, we deployed 19 seismic broadband stations at 1-2 m depth along a 9-km seismic profile from a wind park in Uettingen/Bavaria in order to determine spectral characteristics and amplitude decays of wind-turbine induced seismic signals in the far field.

Average PSD spectra were calculated from 10 min time segments extracted from a continuous data set of up to 6 months. In the frequency range, between 1 Hz and 10 Hz, we identified 7 distinct peaks whose amplitudes correlate with the rotation speed of the wind turbines. These peaks can be observed to at least 4 km distance, lower frequencies even up to the end of the profile. At distances between 300 m and 4 km the PSD amplitude decay can be described by a power law with exponent  $b$ . The measured  $b$ -values exhibit an almost perfect linear frequency dependence and range from  $b = 0.39$  at 1.14 Hz to  $b = 3.93$  at 7.6 Hz.

As an alternative method and to verify the measured PSD amplitude decay, we additionally determined the decay of RMS amplitudes in the time domain at the corresponding peak frequencies. The resulting  $b$ -values are about half as large as in the case of the PSD-amplitudes and also show a characteristic linear frequency dependence. Taking into account the squaring of amplitudes for the PSD calculation, these results confirm the derived  $b$ -values and the robustness of the two approaches.

In a second step, the observed seismic radiation and the measured amplitude decay are modeled using an analytical approach to approximate the surface wave field by also including effects of phase shifts between source signals.

It can be shown that not only the number of wind turbines, the wind-farm geometry and geological properties, but also phase shifts between source signals have significant effects on the interference pattern and amplitude decays. We apply a *phase-shift-elimination-method* to handle the problem of choosing representative source signals as an input for the modeling. This approach can be used to study various effects such as wind farm geometry and source configurations in addition to estimating the expected seismic radiation for different signal frequencies of an arbitrary wind farm. Limitations can arise, if the subsurface exhibits complexities, especially at shallow depth.

Finally, a comparison of modeled and long-term observed amplitude decays with distance for signals with frequencies of 1.14 Hz, 3.5 Hz and 7.6 Hz shows good agreement.

The project KWISS is funded by the Federal Ministry for Economic Affairs and Energy and ESWE Innovations- und Klimaschutzfond.



## **Wind Turbine Noise Reduction from Seismological Data**

Janis Heuel<sup>1</sup>, Wolfgang Friederich<sup>1</sup>

<sup>1</sup>Ruhr-Universität Bochum

Over the last years, installations of wind turbines (WTs) increased worldwide. Owing to negative effects on humans, WTs are often installed in areas with low population density. Because of low anthropogenic noise, these areas are also well suited for sites of seismological stations. As a consequence, WTs are often installed in the same areas as seismological stations. By comparing the noise in recorded data before and after installation of WTs, seismologists noticed a substantial worsening of station quality leading to conflicts between the operators of WTs and earthquake services.

In this study, we investigate options to reduce or eliminate the disturbing signal originating at WTs from records of seismological stations by additionally measuring the WT noise in its immediate vicinity. We hypothesize that highly similar signals emitted by the WT produce similar noise at the seismological station. If this is true, we can predict the noise at the station during an earthquake using data recorded at the WT and the station in the past. To check this hypothesis, we looked for seismological stations in NRW which exhibit a significant correlation between noise power spectral density and hourly windspeed measurements and selected a site close to Haltern am See where we additionally installed low cost seismometers (Raspberry Shake 3D) at surrounding WTs to continuously record WT noise. The newly installed seismometers are dominated by signals of each WT.

To quantify the similarity between signals at the WT, we compute the Euclidean distances of a selected signal and all time windows of the same length in the continuous record. The resulting distance profile represents the Euclidean distance over time and is zero at the location of the selected test signal. We are able to find highly similar signals at the WT by extracting signals corresponding to local minima in the distance profile. We get a noise model at the seismological station from the similar signals which we use to eliminate the disturbing WT noise using Continuous Wavelet Transform. Additionally, we denoise the signal by using the recorded noise before the theoretical first onset. First results show that pre noise denoising leads to improved seismograms and helps to detect hidden events in data recorded at a station that is negatively affected by WTs.

## **3D numerical modelling of windturbine noise: methods of lowering noise levels**

Rafael Abreu, C Thomas

Westfälische Wilhelms-Universität Münster

We numerically test the effect of wind-turbine (WT) locations on the seismic noise generated. By considering different arrangements and number of installed WTs, we find a correlation between location, the number of the WTs and the seismic noise recorded in the vicinity. Surprisingly different arrangements show anti-correlation between the number of WT and noise generated. This suggests that certain arrangement of WT can be used to avoid the seismic noise generated. We measure the predicted wave attenuation with respect to the distance to the WT. This help us to numerically determine the minimum distance that a seismic station need to be located when certain number of WTs are installed. Our numerical simulations allow us to better understand the physics of the wave propagation of wind-turbine noise. We also propose future investigations to design seismic metamaterials filled with volcanic materials to produce enough seismic attenuation in order to avoid the seismic noise in the vicinity of WTs.